

# Modelling polycrystalline semiconductor solar cells

M. Burgelman\*, P. Nollet, S. Degrave

University of Gent, Electronics and Information Systems (ELIS) Pietersnieuwstraat 41, B-9000 Gent, Belgium

## Abstract

An overview is given of various electronic effects present in polycrystalline thin film solar cells, which do not occur in standard crystalline Si solar cells. It is explained how these effects are treated numerically in a numerical solar cell simulation tool, SCAPS, developed at the author's institute. The capabilities and limitations of SCAPS are discussed. Simulation examples of current–voltage, capacitance–voltage and capacitance–frequency characteristics are given. The agreement between the simulations and measurements is shown and discussed, both for CdTe and for Cu(In,Ga)Se<sub>2</sub> solar cells. © 2000 Elsevier Science S.A. All rights reserved.

*Keywords:* Solar cells; Thin film; Modelling; CdTe; Chalcopyrite

## 1. Introduction

Modern, chalcogenide based, thin film solar cells have a quite complicated electronic structure, an example of which is: glass/Mo/two layers of CIGS with a different Ga content/a surface layer of CuIn<sub>3</sub>Se<sub>5</sub>/CdS buffer/two layers of ZnO window. The line-up of the bands can show discontinuities, interface states may be present between the layers, and deep states in the semiconductors may carry charge. These effects can give rise to a fan of effects not encountered in crystalline solar cells such as: roll-over and cross-over of the  $I$ – $V$  characteristics, non-monotonous  $C$ – $V$  characteristics, dispersion in the  $C$ – $f$  characteristics, bias dependence of the spectral response. The complexity of the phenomena mentioned here is such that a realistic prediction of the characteristics is beyond elementary calculations, or the use of ‘rules of a thumb’.

A numerical simulation programme, called SCAPS, was developed at our lab and introduced in the literature [1,2]. The capabilities of this user programme will be briefly reviewed, and recent enhancements will be presented. We will present examples of the modelling capabilities of SCAPS, and its relevance to realistic prediction of the characteristics of CdTe and CIGS based solar cells. We will concentrate on the role of the back contact in CdTe solar cells to the  $I$ – $V$  and  $C$ – $V$  curves, and on the influence of charged interface states on the cross-over of the light and dark  $I$ – $V$  curves in Cu(In,Ga)Se<sub>2</sub> solar cells.

## 2. Cell model

In principle, any numerical program capable of solving the basic semiconductor equations could be used for modelling thin film solar cells. The basic equations are: the Poisson equation, relating the charge to the electrostatic potential  $\Phi$ , and the continuity equations for electrons and holes. In one dimension, the total cell length  $L$  is divided in  $N$  intervals, and the value of  $\Phi_i$  and of the electron and hole concentrations  $n_i$  and  $p_i$  at each of the intervals constitute the unknowns of the problem. They can be found by numerically solving  $3N$  non-linear equations, i.e. the basic equations at each of the intervals  $i$ . Alternatively, one can choose  $\Phi_i$ ,  $E_{Fni}$  and  $E_{Fpi}$  as independent variables instead of  $(\Phi_i, n_i, p_i)$ . Here  $E_{Fni}$  and  $E_{Fpi}$  are the quasi-fermi energy levels for electrons and holes respectively. The basic equations are non-linear because the continuity equations contain a recombination term, which is non-linear in  $n$  and  $p$ .

Several additional requirements must be met if the program is to simulate thin film polycrystalline solar cells realistically. It must allow for multiple semiconductor layers; six layers are needed in the example given in the introduction section. At the interfaces between the layers, discontinuities in the energy bands  $E_C$  and  $E_V$  and hence in the band gap  $E_g$  can be present and interface recombination can occur. A solar cell simulation program should be able to handle this. It should also correctly treat the problem of recombination and charge in deep states in the bulk of the layers. It should be able to calculate and simulate the relevant electro-optical measurements commonly carried out on thin film solar cells, this is: not only the  $I$ – $V$  characteristics, but also the spectral response  $Q(\lambda)$  and the capacitance

\* Corresponding author. Tel.: +32-9264-3381; fax: +32-9264-3594.  
E-mail address: burgelman@elis.rug.ac.be (M. Burgelman)

measurements  $C-V$  and  $C-f$ , preferably all these as a function of ambient temperature. Finally it should provide convergence at least for the most common thin film cell structures, say, at least for basic TCO/CdS/CdTe and CIGS/CdS/TCO structures at normal working conditions. This is sometimes a weak point for a program dedicated to the simulation of silicon cells, due to the occurrence of large band gap materials in typical thin film cells. We discuss now how these features are implemented in our simulation program SCAPS (solar cell capacitance simulator) [1,2].

### 2.1. Deep bulk levels

In each layer, the type (donor or acceptor) and density of one shallow level can be defined; it is completely ionized and does not contribute to recombination. Also, up to three deep levels can be defined. Recombination in these levels and their occupation, is described by the Shockley–Read–Hall (SRH) formalism, and charge is defined by the occupation of the level and its type (donor or acceptor, or ‘neutral’, i.e. a hypothetical center carrying no charge). The levels can be energetically distributed in the forbidden zone (single level, uniform band, Gauß, or exponential tail). The concentration of the shallow or deep states can vary spatially (uniform, step, linear or exponential). Auger recombination is not treated, but is a straightforward extension. Amphoteric states, i.e. states with three or multiple charge and energy states, cannot be handled for the moment. Their implementation however is straightforward, and would extend the applicability of our program to amorphous cells. Conduction through deep states (hopping) is not implemented.

### 2.2. Interface states and band discontinuities

The quasi-fermi levels are allowed to be discontinuous at the interfaces. To handle this mathematically, an extra node at each interface is introduced in the discretization [2]. The relation between fermi level discontinuity, carrier concentrations and current is given by the expressions for thermionic current at the interface [2,3]. Recombination at the interface states and their occupation, is described by an extension of the SRH formalism, allowing the exchange of electrons between the interface state and the two adjacent conduction bands, and of holes between the state and the two adjacent valence bands (Fig. 1) [4,5]. This assumption is crucial in the case illustrated in Fig. 1, since the dominant recombination term in this case is between electrons of the semiconductor on the left and holes in the semiconductor on the right side of the interface. Other simulation programs are only treating recombination within the same layer: PC-1D [6], ADEPTF [7] and AMPS [8]. An extra, dummy layer has to be introduced to handle the case of Fig. 1 correctly, i.e. a very thin layer whose conduction band levels with  $E_C$  of the left layer, and whose valence band levels with  $E_V$  of the right

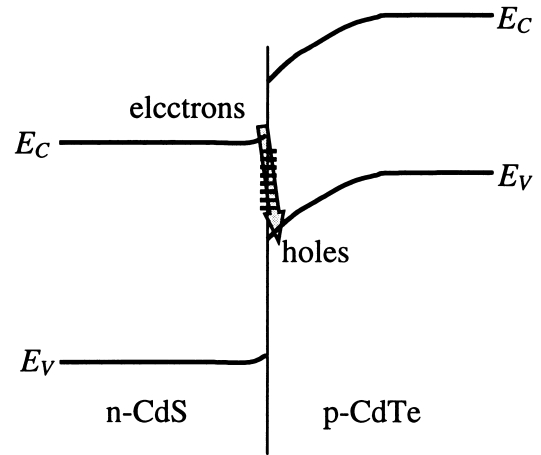


Fig. 1. Model for interface recombination. In this case, relevant for a CdS/CdTe cell, the dominant recombination path is between window electrons and absorber holes.

layer. In our SCAPS program, the interface states can be distributed in energy, in the same way as are the bulk states.

At the metal–semiconductor interfaces (contacts), transport of majority carriers is described by thermionic emission (Bethe theory [9]). Transport of minority carriers is described by their surface recombination velocity  $S_n$  or  $S_p$  at the contact.

Tunnelling at interfaces or at contacts is not implemented in SCAPS.

### 2.3. Optical generation

SCAPS can handle steady state illumination by monochromatic light or by light of a standard spectrum (AM1.5G and AM1.5D are implemented by default). The wavelength region can be limited to simulate the use of long pass and short pass filters. Above that, a ‘small signal’ illumination can be added to simulate a spectral response measurement. An exponential absorption law, characterized by a few user parameters, is assumed for all semiconductor layers. Extension to a completely user defined  $\alpha(\lambda)$  law is straightforward. The implementation of optical layers, which don’t have an electronic effect, but which introduce a user defined transmission  $T(\lambda)$ , will be implemented in the near future. No interference phenomena or optical confinement (texture and ray tracing) are handled at present.

### 2.4. Steady-state (d.c.) simulations

The steady-state semiconductor equations are discretized according to the exponential fitted finite difference scheme and solved by the Gummel iteration scheme [10]. The variations of the variables in one iteration cycle are limited to a user set value (clamping). An own choice of independent variables and a suitable normalization of all variables, was a key issue in obtaining convergence for typical thin film cells at normal working conditions [2]. Nevertheless, convergence at high forward voltages remains

a weak point, as it also is in most other simulation programs. Also, SCAPS does not perform well when multiple junctions (pnp, pnnp etc. structures) are to be simulated. This is in part due to inherent assumptions in SCAPS (choice of variables, initial guess etc.).

### 2.5. Alternating-current (a.c.) simulations

When a steady state calculation converges, SCAPS can carry out a small signal analysis around the d.c. operating point, yielding the complex admittance i.e. the capacitance  $C$  and the conductance  $G$ . This is done by an elegant method [2] where the coefficient matrix of the equations describing the problem is rearranged such that it forms an (almost) tridiagonal matrix in which each element is in itself a  $3 \times 3$  matrix. The system is linear and can be solved without iteration for any frequency, provided, of course, that the d.c. solution is known.

As it is now, SCAPS does not perform calculations in the time domain. It is thus unable to calculate transient phenomena.

## 3. The simulation program SCAPS

SCAPS is a Windows application program, developed at the university of Gent with LabWindows/CVI of National Instruments. It has been made available to university researchers in the photovoltaic community after the second PV World Conference in Wien, 1998. A solar cell simulation problem is stored in an ASCII file, which can be read and completely edited by the graphical user interface of SCAPS. The program is organised in a number of panels (or windows or pages in other jargon), in which the user can set parameters or in which results are shown. The program opens with an 'action panel', where the user can set an operating point (temperature, voltage, frequency, illumination), and an action list of calculations to carry out ( $I-V$ ,  $C-V$ ,  $C-f$ ,  $Q(\lambda)$ ). In each calculation, the running parameter ( $V$ ,  $f$  or  $\lambda$ ) is varied in the specified range, whilst all other parameters have the value specified in the operation point. One can also load or edit a problem file. The user can navigate to many auxiliary panels. One, in which the parameters for one defect level in one layer are set, is illustrated in Fig. 2. Also, the user can directly view previously calculated results:  $I-V$ ,  $C-V$ ,  $C-f$ ,  $Q(\lambda)$ , but also band diagrams, electric field, carrier densities, partial recombination currents i.e. pertaining to one single mechanism. An example of such a results panel is given in Fig. 3. All calculations can be saved in ASCII format, to be handled by the user with their preferred toolkit.

SCAPS version 2.1, which is available now, has some enhancements over version 2.0, which was made available after the Wien Conference.

- Convergence is improved: the termination criteria for the

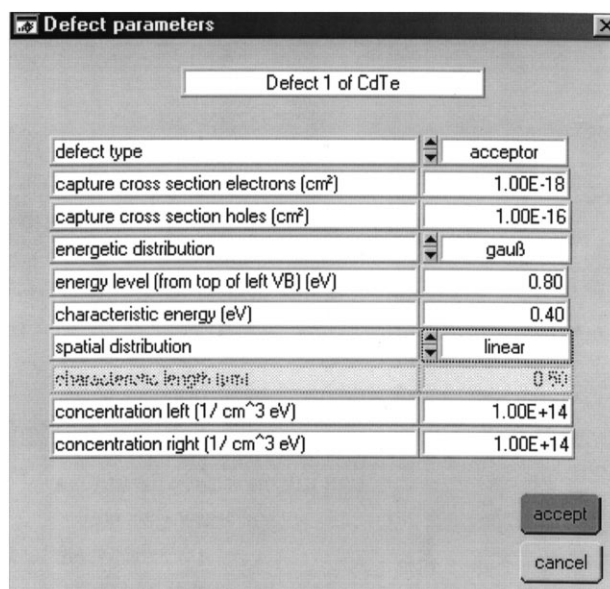


Fig. 2. Typical data input panel of the SCAPS graphical user interface, allowing to set the parameters of one particular defect level in one particular layer.

electrostatic potential and the two fermi-levels can now be edited by the user.

- When divergence occurs, the points calculated so far are not lost, but are shown.
- A status line informs the user about the progress of the calculation, and of the status after its termination.
- The possibility of illumination from either the p side or the n side is now built in.
- The solar cell parameters  $V_{oc}$ ,  $J_{sc}$ ,  $FF$  and  $\eta$  are calculated by interpolation of the calculated  $I-V$  points.
- Many graphs can be shown on a logarithmic or a linear scale, by a click (see Fig. 3).
- After calculation, the data are displayed on screen by a simple click. Parts of it can be cut and pasted to other application programs, such as spreadsheets.
- The quality of the graph printing is greatly improved.

## 4. Modelling of CdTe thin film solar cells

Two important research topics relevant to CdS/CdTe solar cells are: the influence of the  $CdCl_2$  treatment and the influence of the back contact on the CdTe layer. Both phenomena are recognised to strongly influence the cell behaviour. Much research was carried out on these subjects, and understanding of the underlying physical phenomena is now beginning to emerge. We illustrate here how SCAPS has been used in this field.

Striking features of the  $I-V$  characteristics of a thin film CdS/CdTe solar cell are the roll-over and the cross-over of the  $I-V$  curves. Roll-over is the phenomenon that an  $I-V$  curve shows a kink and the current levels of at higher voltage. Cross-over is the phenomenon that the dark and

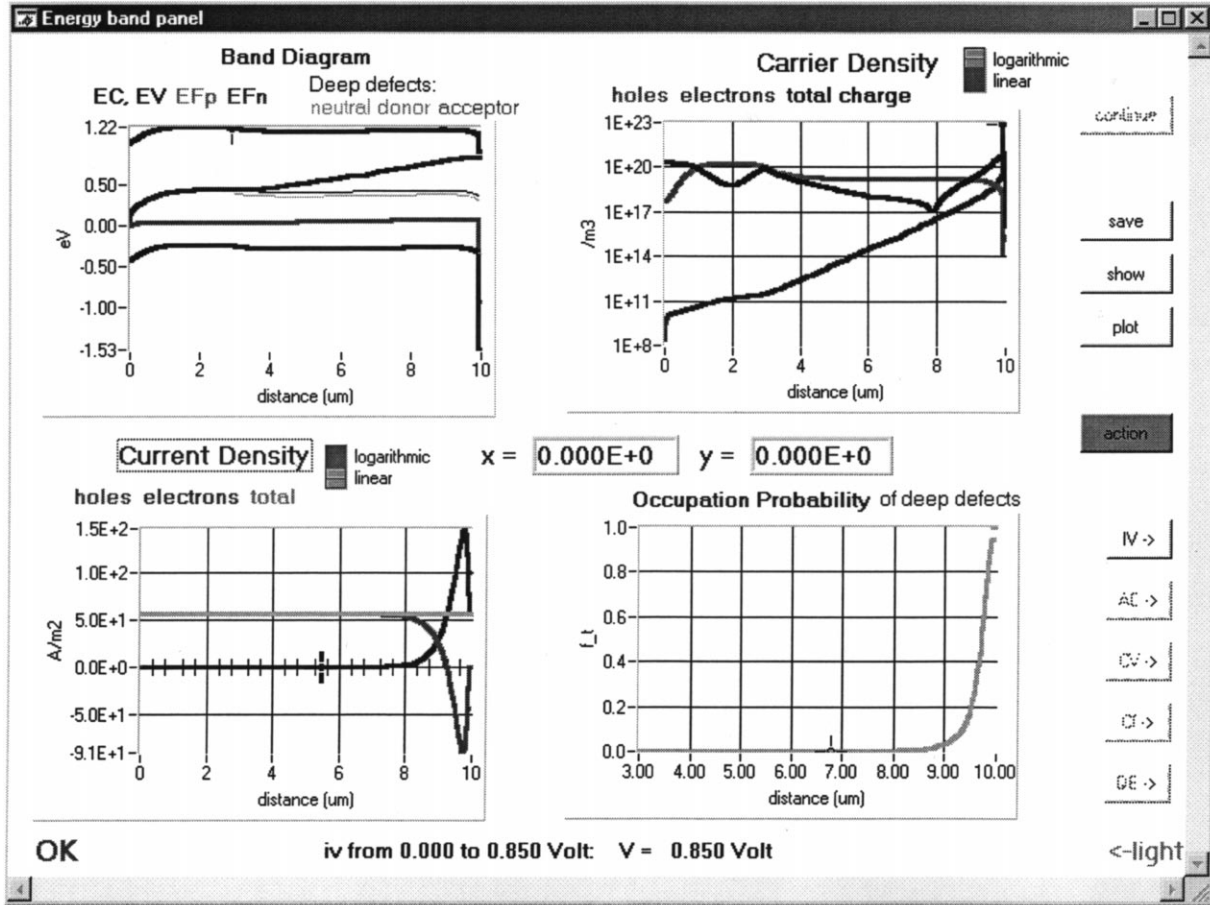


Fig. 3. An example of a SCAPS panel displaying calculated results: ‘energy band panel’. The example shown is for an illuminated CdS/CdTe solar cell at forward voltage.

illuminated  $I-V$  curves intersect. Roll-over is easily explained by the assumption that the back contact of the CdTe layer behaves as a rectifying Schottky contact, which is reverse biased when the CdS/CdTe solar cell is at forward bias [1,11,12]. This simple model of two diodes back-to-back can explain the gross features of the  $I-V$  curves: It predicts that the  $I-V$  curves level off at the reverse saturation current of the Schottky contact back contact; measurement of the thermal activation energy of this saturation current yields the contact barrier [11]. It was realised that the simple model also explains an unusual feature of the  $C-V$  curves measured at forward bias: the capacitance  $C$  does not increase monotonously with bias voltage  $V$ , but it shows extrema, e.g. two maxima and one minimum [1,12]. This feature was used to measure the doping density in the CdTe layer both at positions close to the junction with CdS and at positions close to the back contact. It is far more difficult to explain the cross-over phenomenon. In Ref. [12] it was explained by making an estimate of the electron current in the CdTe layer close to the back contact. This explanation critically relies on several assumptions, e.g. about the minority carrier diffusion length. It is beyond intuitive insight or rules of a thumb to quantify the effects

of such assumptions to the various solar cell characteristics that can be measured. A realistic simulation tool, such as SCAPS, is needed.

Figs. 4–6 illustrate the qualitative agreement between measured and simulated  $C-V$  and  $I-V$  curves for cells with an Au back contact. While the gross form of the  $C-V$  curves can be explained by a simple two diode model, the calculation  $I-V$  curves requires a sophisticated and dedi-

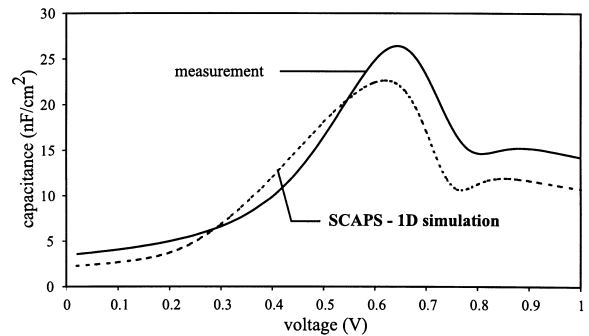


Fig. 4. Measured and simulated  $C-V$  curves of a CdS/CdTe/Au solar cell, at forward voltages. The occurrence of maxima in this curve is indicative for a contact barrier.

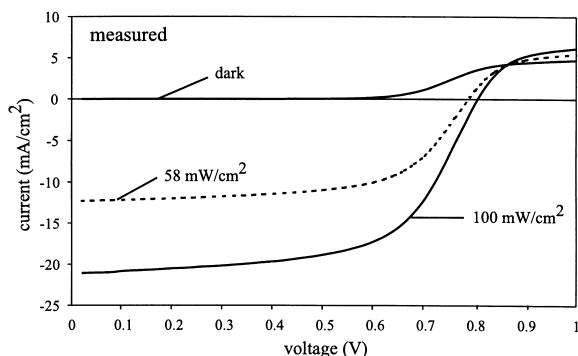


Fig. 5. Measured  $I$ - $V$  curves of a CdS/CdTe/Au solar cell, for varying illumination intensity.

cated numerical simulation tool. Recent measurements on CdTe cells with a  $\text{Sb}_2\text{Te}_3$  contact layer show that the cross-over effect strongly depends on the wavelength of the illumination: it is only provoked by light of near band gap energy [13]. The assumptions that have lead to Fig. 6 are not valid in this case, and further modelling work is needed to explain these observations quantitatively.

Measurement of the capacitance of the cells as a function of frequency ( $C$ - $f$  curves, Fig. 7) show considerable frequency dispersion, which increases with increasing degree of  $\text{CdCl}_2$  treatment [14]. A standard explanation for such behaviour is the occurrence of a broad band of deep acceptor states. The insertion of such a band of levels in SCAPS (implemented in an input panel as illustrated, e.g. in Fig. 2) leads to simulated  $C$ - $f$  curves which qualitatively agree with the measurements (Fig. 8). By comparing the measured and simulated curves (Figs. 7 and 8), one sees that an increasing 'degree of  $\text{CdCl}_2$  treatment' is modelled by an increasing density of deep acceptor states. Such a model will only acquire credibility if it is capable to explain other measured characteristics, with the same input parameter set. It was shown in [14] that the influence of  $\text{CdCl}_2$  treatment on the measured spectral response is quite well simulated. In [15] it is shown that the same assumptions also allow simulating the observed apparent doping profile in the CdTe layer next to the junction with CdS.

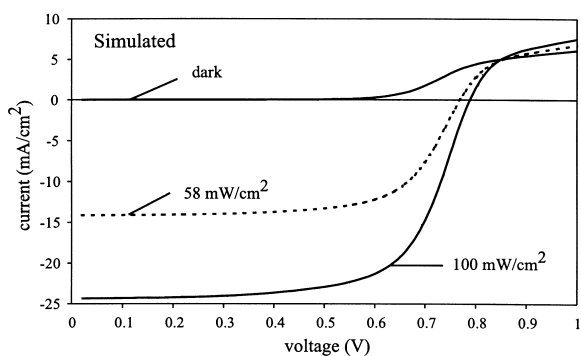


Fig. 6. SCAPS simulation of the  $I$ - $V$  curves of a CdS/CdTe/Au solar cell, for varying illumination intensity.

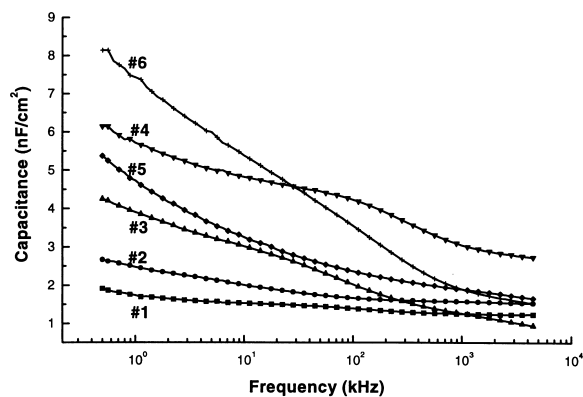


Fig. 7. Measurement of  $C$ - $f$  curves of CdTe solar cells with varying 'degree of  $\text{CdCl}_2$  treatment' (numbering in increasing degree of treatment).

## 5. Modelling of CIGS thin film solar cells

State-of-the art CIGS cells have a complex multilayer structure. It is often assumed that a thin layer of an ordered defect compound (ODC, supposedly  $\text{Cu}(\text{In,Ga})_3\text{Se}_5$ ) is formed at the surface of the CIGS layer, next to the CdS buffer layer [16]. The electronic properties of this layer are beyond direct measurement in a completed cell structure. Cell analysis is also complicated by a complicated window structure, consisting of a thin buffer layer (CdS or an alternative) and a double TCO layer (e.g. nominally undoped ZnO followed by Al doped ZnO). It is clear that numerical modelling is necessary to evaluate quantitatively the effect of a set of assumed input parameters.

In Fig. 9 the  $C$ - $f$  characteristics of a  $\text{Cu}(\text{In,Ga})\text{Se}_2$  thin film solar cell are measured as a function of ambient temperature. The frequency dispersion observed at temperatures above 200 K, i.e. the gradual decrease of capacitance over several decades of frequency again is explained by assuming a band of deep acceptor states in the  $\text{Cu}(\text{In,Ga})\text{Se}_2$  depletion region. The step in the  $C$ - $f$  curves at temperatures below 160 K is explained by assuming donor type interface states at the ODC/CdS interface, energetically distributed

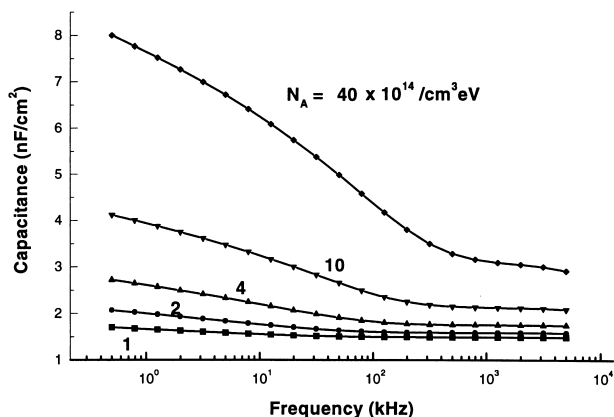


Fig. 8. SCAPS simulation of  $C$ - $f$  curves of CdTe solar cells with varying density of deep acceptor states in the CdTe layer.

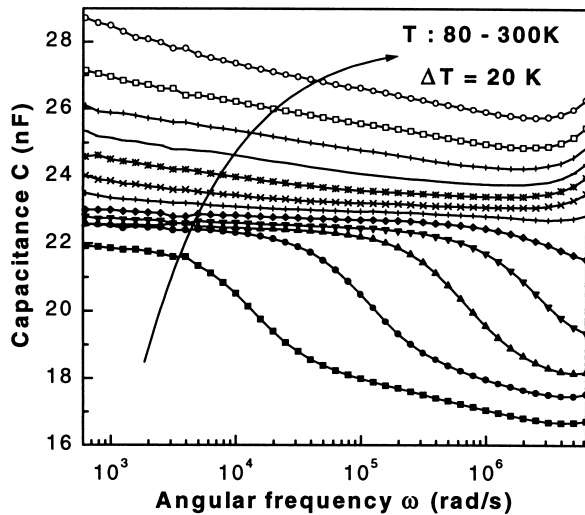


Fig. 9. Measured  $C$ - $f$  curves of a CIGS solar cell in the temperature range 80–300 K (20 K steps).

over the whole energy gap [17]. The resulting SCAPS simulation of the  $C$ - $f$  curves is shown in Fig. 10; it agrees well with the measured curves of Fig. 9. When in addition a high density of acceptor type defects is assumed in the ODC layer, also the crossing-over of the  $I$ - $V$  characteristics can be simulated fairly well [17].

## 6. Conclusion

The examples given above illustrate the numerical simulation program SCAPS is a valuable tool in modelling polycrystalline thin film solar cells based on CdTe and on CIGS. Comparison between measured and simulated characteristics can lead to a better insight in the internal physical operation of a solar cell, as was illustrated in the examples given above. It is however clear that measurement/simulation plots as those of Figs. 9 and 10 are not to be considered as a real ‘proof’ that the cell under investigation has an electronic structure as assumed in the simulation. The fan of possible input parameters is so wide that one cannot be sure that there does not exist another set of parameters which will yield agreement between measurement and calculation which could be judged equally well as the one in Figs. 9 and 10. As many as possible kinds of measurements and simulations should be carried out on the same cell. As a rule, both current and admittance measurements should be carried out, when possible under a varying excitation (temperature, illumination etc.). Also, the choice of the input parameter set should be guided by the outcome of independent non-electrical measurements (e.g. all kinds of spectroscopy) on completed and partial cell structures.

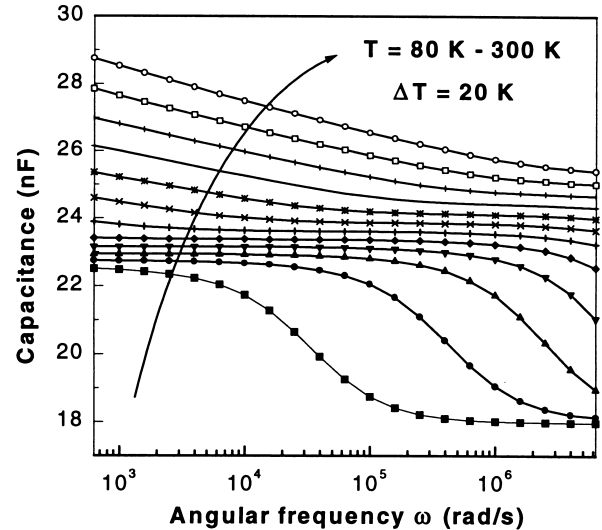


Fig. 10. SCAPS simulation of  $C$ - $f$  curves of a CIGS solar cell in the temperature range 80–300 K (20 K steps).

## References

- [1] A. Niemegeers, M. Burgelman, Proc. 25th IEEE Photovoltaic Spec. Conf., Washington DC, IEEE, New York, 1996, pp. 901–904.
- [2] A. Niemegeers, S. Gillis, M. Burgelman, 2nd World Conf. Photovoltaic Energy Conv., Wien, Österreich, July 1998.
- [3] S. Fonash, Commun. Solid State Electr. 22 (1979) 907.
- [4] H. Pauwels, G. Vanhoutte, J. Phys. D.: Appl. Phys., 11 (1978) 649.
- [5] M. Burgelman, A. De Vos, A. Niemegeers, Proc. 12th Eur. Photovoltaic Sol. Energy Conf., Amsterdam, The Netherlands, April 1994, Stephens, UK, pp. 1557–1560.
- [6] P.A. Basore, IEEE Trans. Electron Dev. 37 (1990) 337.
- [7] Y. Lee, J. Gray, Proc. 12th Euro. Photovoltaic Sol. Energy Conf., Amsterdam, The Netherlands, April 1994, Stephens, UK, pp. 1561–1564.
- [8] P. McElhany, J. Arch, J. Appl. Phys. 64 (1988) 1254.
- [9] E. Rhoerick, Metal-Semiconductor Contacts, Clarendon Press, Oxford, 1978.
- [10] S. Selberherr, Numerical Analysis of Semiconductor Devices, Springer Verlag, Wien, 1984.
- [11] G. Stollwerck, J.R. Sites, Proc. 13th Eur. Photovoltaic Sol. Energy Conf., Nice, France, October 1995, Stephens, UK, pp. 2020–2022.
- [12] A. Niemegeers, M. Burgelman, J. Appl. Phys. 81 (1997) 2881.
- [13] P. Nollet, M. Burgelman, S. Degraeve, Thin Solid Films (this issue) 361–362 (2000) 293.
- [14] A. Niemegeers, M. Burgelman, H. Richter, D. Bonnet, Proc. 14th Euro. Photovoltaic Sol. Energy Conf., Barcelona, Spain, July 1997, Stephens, UK, pp. 2079–2082.
- [15] M. Burgelman, P. Nollet, S. Degraeve, Appl. Phys. A 69 (1999) 149.
- [16] D. Schmid, M. Rukh, F. Grünwald, H.-W. Schock, J. Appl. Phys. 73 (1993) 2902.
- [17] A. Niemegeers, M. Burgelman, R. Herberholz, U. Rau, D. Hariskos, H.-W. Schock, Prog. Photovoltaics 6 (1998) 407–421.